Adaptive Model Predictive Control Based Frequency Regulation for Low-inertia Microgrid

Weichao Wang, Yutaka Sasaki, Naoto Yorino, Yoshifumi Zoka, Ahmed Bedawy
Graduate School of Advanced Science and Engineering
Hiroshima University
Higashi-hiroshima, Japan
wang-weichao@hiroshima-u.ac.jp

2023 5th International Conference on Power and Energy Technology (ICPET) | 979-8-3503-3967-3/23/$31.00 ©2023 IEEE | DOI: 10.1109/ICPET59380.2023.10367501

***Abstract*—Large amount of renewable energy sources affect frequency stability in microgrid (MG) This paper proposes a novel frequency regulation method based on adaptive model predictive control (AMPC) for MG system considering large disturbances to maintain the frequency stability. The MG system performance is approximated by a simplified first-order lag internal prediction model (IPM), which is applied to AMPC. Parameters of the IPM are estimated and updated by unscented Kalman filter (UKF) in real-time. Therefore, an optimal control operation can be obtained to cope with the MG system frequency problem caused by uncertainty of the disturbances, such as wind turbine (WT) power, photovoltaic (PV). An isolated MG model with high penetration of PV, WT, and battery energy storage system (BESS) is used to verify the performance of the proposed AMPC method under low inertia circumstance. The simulation results show that the proposed method has better performance than the PI controller. Moreover, AMPC including UKF can treat low inertia MG system operation without frequency instability.**

Keywords—microgrid system, frequency regulation, renewable energy source, adaptive model predictive control, unscented Kalman filter

I. INTRODUCTION

Renewable energy sources, such as wind turbine (WT) and photovoltaic (PV), is increasingly being used, as it can reduce carbon emissions. Microgrid (MG) system are attracting attention due to a large amount of renewable energy installed. System operation would be quite challenging due to the uncertainty and unpredictable nature of the renewable energy sources. However, the installation of large amounts of renewable energy sources can reduce system inertia and potentially lead to system instability, especially frequency instability. Load frequency control (LFC) is an essential technique to maintain the frequency into the desired range.

Therefore, MG systems with large amount of WT, PV require high robustness and fast response for LFC controller to maintain the frequency stability. Recently, many researchers review the recent trends of power systems and state-of-the-art techniques for the design of the LFC controller [1]-[3]. The simple PI controller wildly used to design the LFC controller due to its simple configuration. However, the parameters of PI controller must be tuned when the system characteristics change. Based on this point, many optimization algorithms, such as chaotic atom search optimization, coyote optimization are used to design the LFC controller, which can estimate the controller parameters [4], [5].

The frequency stability of the MG system is critical to prevent power outages. The uncertainty of WT, PV, and load is main causes of frequency instability . Many researchers consider the influence of uncertainty of renewable energy sources in designing of LFC controller. Some papers report that the performance of the LFC can be improved by using the battery energy storage system (BESS). Authors in [6] propose a two-layer optimization strategy for BESS to improve the frequency regulation performance. Authors in [7] discuss the performance of frequency response strategies considering the high penetration of renewable energy sources. Authors in [8] discuss the various recent storage technologies have been applied to handle the uncertainty problem, such as super-conducting magnetic energy storage, flywheel energy storage, and redox flow batteries. A optimal control method based on sliding mode control is proposed in [9] considering the renewable energy and time delay. Some intelligent algorithm, such as fuzzy logic, reinforcement learning, neural network also used to design the LFC controller [10]-[12]. Although the simulation results of these techniques exhibit high performance to cope with the frequency problem, but they require a lot of computational time to obtain the optimal operation.

This paper propose a novel adaptive MPC (AMPC) method for MG system frequency regulation using unscented Kalman filter (UKF). UKF is also applied to estimate the state variables and parameters, which is reported by [13]-[15]. The proposed AMPC using a simplified first-order lag model as an internal prediction model (IPM) to decrease the computational time. The IPM is used to approximate the performance of the MG system. To observe the system dynamic, an UKF is applied to AMPC. In the proposed configuration, UKF can estimate and update the parameter of the IPM online. An optimal control operation can be obtained in this process. An isolated MG system with large disturbance and high penetration of PV, WT, and BESS is used to identify the effectiveness of proposed AMPC method. The simulation results show that the proposed AMPC method can effectively address the MG frequency problem and exhibit a better performance than the PI controller.

The other parts of this paper are described as follows. First, section II discusses the design of the AMPC controller for the MG system. Then, system conditions and simulation results are given in section III. Finally, section IV gives the conclusions of this paper.

II. The Design of the Proposed AMPC Method for MG

A. MG System

This paper assumes an MG equivalent frequency response model represents the actual system. This system includes the governor model, the diesel engine generator (DEG) model, the BESS model, and the frequency characteristic model of the MG, as shown in Fig. 1. A dynamic state-space equation is presented for the MG system, which is used to design the AMPC controller, as shown in (1), (2).

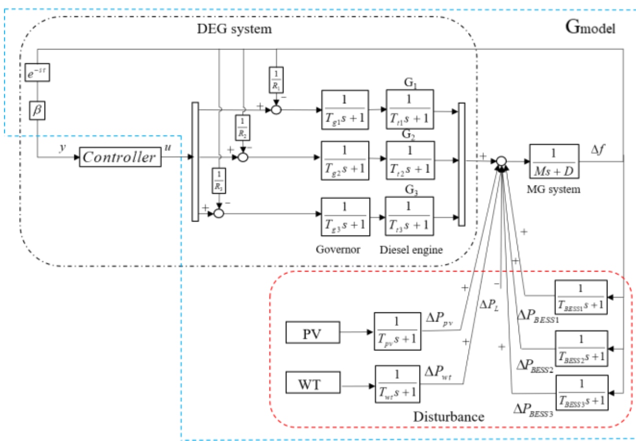

Fig. 1. MG system model.

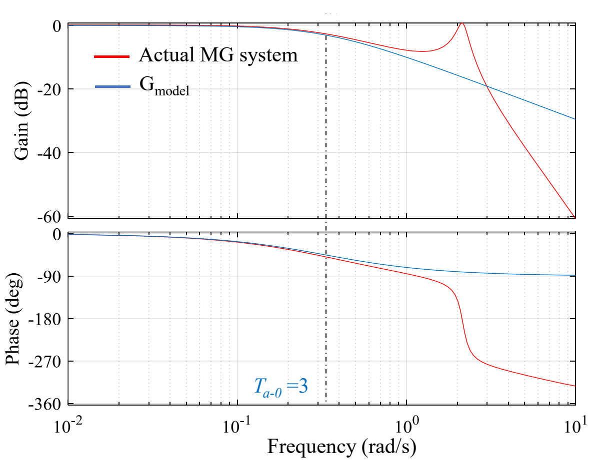

Fig. 2. Bode plot.

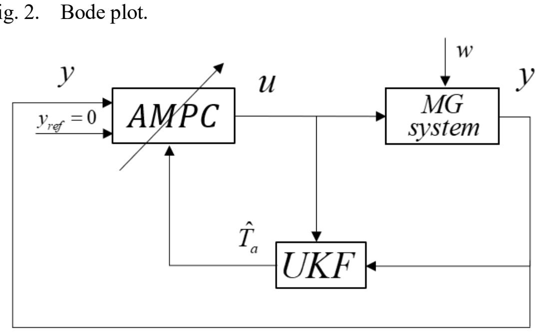

Fig. 3. The structure of AMPC using UKF.

$$\begin{aligned} x(k+1) &= \boldsymbol{A}x(k) + \boldsymbol{B}u(k) + \boldsymbol{E}w(k) \\ y(k) &= \boldsymbol{C}\,x(k) \end{aligned} \tag{1}$$

$$x_i(k) = \begin{bmatrix} \Delta P_g(k) & \Delta P_t(k) & \Delta f(k) \end{bmatrix}^T \tag{2}$$

where, $\boldsymbol{A} \in \mathbb{R}^{N \times N}$, $\boldsymbol{B} \in \mathbb{R}^{N \times N_B}$, $\boldsymbol{C}^T \in \mathbb{R}^{N \times 1}$, and $\boldsymbol{E} \in \mathbb{R}^{N \times 1}$ are the state-space matrices, N is the number of the state valuables, N_B is the number of the input signal; $x \in \mathbb{R}^{N \times 1}$ is the state valuables of the system; w is the disturbance and load; y and u are the system output and input signal; ΔP_g, ΔP_t, and Δf are the governor output deviation, diesel engine output deviation and frequency deviation; k is the sample moment; τ is equivalent to a communication time delay for the actual control system ($\tau = 0.1s$).

The behavior of WT power, PV generation, and BESS is approximated by the first-order lag system model, shown in (3).

$$Output: \Delta P_m = \frac{1}{T_m s + 1} \times input,\ m = PV, WT, BESSs \tag{3}$$

where, T_{pv}, T_{wt}, and TBESS are the time constant of the PV, WT, and BESSs, respectively.

In the LFC scheme, the generation balance with the load consumption is required. Therefore, the generation and load consumption balance in (4) can be obtained based on this point.

$$\Delta P_t + (\Delta P_{BESS}^{+} - \Delta P_{BESS}^{-}) = \Delta P_L - \Delta P_{pv} - \Delta P_{wt} \tag{4}$$

where, and are the power discharge and charge of BESS; ΔP_L is the load consumption; ΔP_{pv} is the PV output; ΔP_{wt} is the WT output.

A large amount of WT, PV generations, and load consumption affects the frequency stability. Therefore, a fast response BESS is used as a supplementary power to maintain the balance, which is charged and discharged to mitigate the rapid fluctuation.

B. Proposed AMPC Method Using UKF

A simplified first-order lag system as an IPM is applied to AMPC. The performance of the system can be approximated, as in (5). Therefore, AMPC controller can predict future performance based on the internal prediction model (G_{model}).

$$G_{\text{model}}(s) = \frac{1}{T_a s + 1} \tag{5}$$

where, T_a is the time constant of the proposed internal prediction model.

Fig. 2 shows the bode plot of the proposed internal prediction model and the MG system, which is used to decide the initial values of the proposed first-order internal prediction model. We can observe that the proposed first-order system model has a fast response speed and suitably approximate the performance of the MG system in the frequency range of less than 0.33Hz ($1/T_{a-0}$). Fig. 3 shows the structure of how the UKF uses the measurements (u, y) from the MG system for online estimation to obtain the optimal parameter of (5).

C. Rolling Optimization

The proposed AMPC method depends on the updated prediction model to predict the future performance in the prediction horizon (N_p) and obtain the input signal u in the control horizon (N_c). Similarly, the performance of AMPC and the computational burden also depend on the length of prediction and control horizon.

The MPC is an optimality approach for minimizing the objective function. The objective function in (6) is used in the proposed AMPC method to satisfy the frequency range and minimize the control cost.

$$\min J = \sum_{h=1}^{N_p} x(k+h\,|\,k)^T \boldsymbol{Q}\, x(k+h\,|\,k) + \sum_{h=0}^{N_c-1} \Delta u(k+h\,|\,k)^T \boldsymbol{S}\, \Delta u(k+h\,|\,k) \tag{6}$$

where, $\boldsymbol{Q} \in \boldsymbol{C}^T \boldsymbol{C}$ and $\boldsymbol{S} \in 0.1 \cdot \boldsymbol{I}_{Nc\times Nc}$ are the weight matrices of the state valuables and input signal deviation; h is the sample period.

To consider the safe operation and the desired frequency deviation range. The following constraints are also used in the proposed AMPC.

$$\begin{cases} \Delta f^{\min} \le \Delta f(k) \le \Delta f^{\max} \\ u^{\min} \le u(k) \le u^{\max} \end{cases} \tag{7}$$

TABLE I. PARAMETERS OF MG SYSTEM

D (pu/Hz)	M (pu s)	β (pu/Hz)	R_1 R_2 R_3 (Hz/pu)	T_{g1} T_{g2} T_{g3} (s)	T_{t1} T_{t2} T_{t3} (s)
0.012	0.200	0.345	3.0 3.0 3.0	0.20 0.20 0.16	1.1 1.1 0.7

TABLE II. PARAMETERS OF BESS, PV, WT

$T_{BESS,1}$ (s)	$T_{BESS,2}$ (s)	$T_{BESS,3}$ (s)	T_{PV} (s)	T_{WT} (s)
0.100	0.110	0.130	1.8	1.5

TABLE III. CASE SETTING

	System model	Variable renewable
Case A	Fig. 1 (M=0.200, D=0.012 with G_1, G_2, G_3 diesel engine generators)	$\Delta PV_1 + \Delta PV_2$ $\Delta WT_1 + \Delta WT_2$
Case B	Fig. 1 (M=0.150, D=0.010 with G_1 diesel engine generator)	$\Delta PV_1 + 2\times\Delta PV_2$ $\Delta WT_1 + 2\times\Delta WT_2$

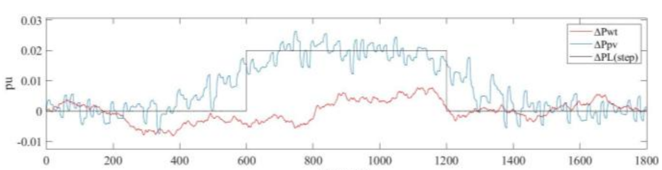

(a). WT_1, PV_1 output and step change.

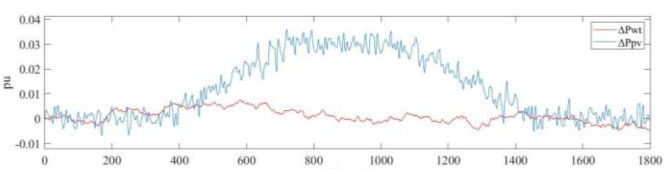

(b). WT_2, PV_2 output.

Fig. 4. WT, PV output and step change.

III. SIMULATION

A. Setting of the AMPC Parameters

The proposed AMPC method and the simulation environment are built using MATLAB/Simulink R2021b software. The initial parameters of (5) are set to $T_{a\text{-}0}$=3 through the bode plot of Fig. 2. N_p=10, N_c=2 with sampling time 0.1s are applied to the AMPC. A PI controller with optimal parameters (K_P=0.02, K_I=-0.1) is used to compare with the proposed AMPC method. The parameters of proportional (K_P) and integral (K_I) are chosen by checking the frequency response of the system. The total capacity of the MG is assumed to be 5MW (1pu).

B. Case Study

The proposed AMPC method is confirmed in an isolated MG systems, whose parameters are summarized in Table. I and II. Case setting is given in Table III. In case A, we assume that the MG system with high penetration of the renewable energy source and large step disturbance during cloudy weather. In case B, when a large amount of PV, and WT is imported into the MG system, and diesel engine G_2 and G_3 in Fig. 1 have stopped generating power during sunny weather, because of the PV generation is increasing in this circumstance. However, it can decrease the system inertia and potentially lead to system instability. Therefore, it is necessary to consider the influence of a large amount of PV and WT imported in MG system. meanwhile the effectiveness of proposed method must be determined in this case. In those case, 0.02pu step change at 600s and -0.02pu step change at 1200s are also shown in Fig. 4(a). Figs. 4(a), (b) also show the PV and WT output to consider the different periods frequency and amplitude. This is an important point due to the PV and WT output can be affected by the weather. Finally, the simulation time is set to 1800s.

C. Simulation Results

Fig. 5 gives the simulation results of frequency deviation for case A. We can observe that the frequency deviation occurs a fluctuation at 0s due to the initial estimation parameters, but it converges quickly. The proposed AMPC method perform a fast response when the step disturbance is imported at 600s and

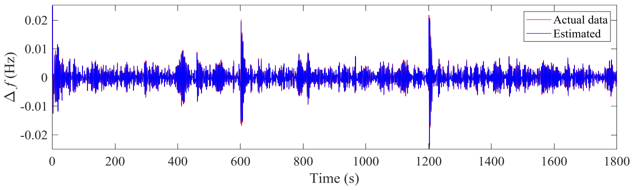

Fig. 5. Frequency deviation in case A.

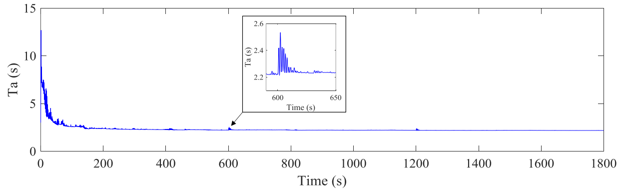

Fig. 6. Estimation parameter by UKF in case A.

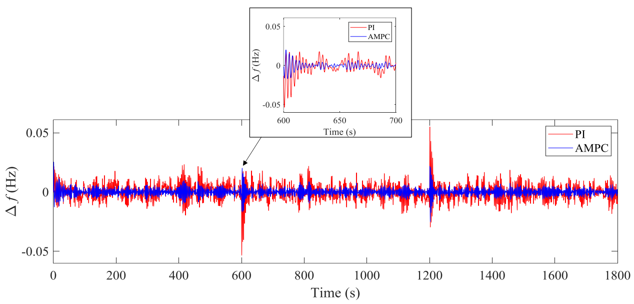

Fig. 7. Comparative results based on case A.

TABLE IV. COMPARISON ANASYNIS BASED ON CASE A

(Hz)	PI	AMPC
Min.	-0.0534	-0.0250
Max.	0.0550	0.0253
STD	0.0066	0.0028

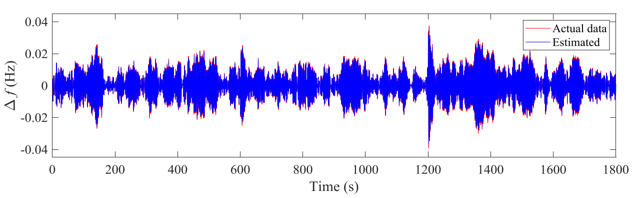

Fig. 8. Frequency deviation in case B.

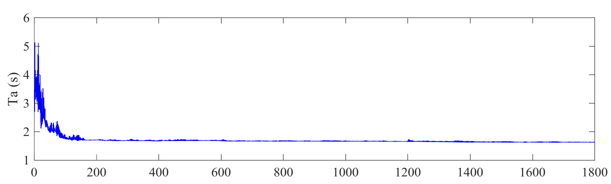

Fig. 9. Estimation parameter by UKF in case B.

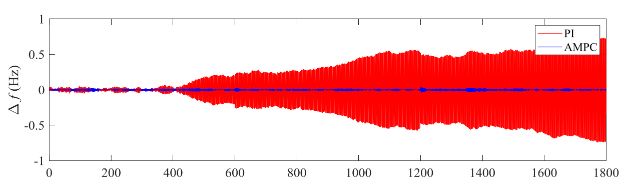

Fig. 10. Comparative results based on case B.

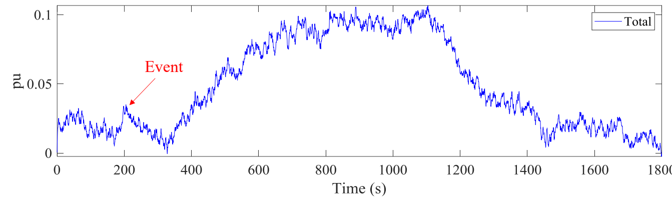

Fig. 11. Total capital of PV and WT in case B.

1200s and rapidly convergence to the desired range. There is a small estimation error between actual data and estimated state variables by UKF. The simulation results show that the proposed AMPC method can effectively cope with the frequency problem.

Fig. 6 shows the results of estimation parameter by UKF. We can observe that the estimation parameter occurs a fluctuation from 0s to almost 40s to obtain the optimal parameter for MG system, and stables at a constant value $T_a \approx 2.21$. The enlarged plot in Fig. 6 also shows that the UKF can estimate the optimal parameters to address the system dynamic fluctuation. UKF performs a high estimation accuracy and fast speed when the step change is imported.

Fig. 7 shows the comparative results based on case A, whose comparative data of frequency deviation using minimization (Min.), maximization (Max.), and standard deviation (STD) indices is given in Table IV. Form the results, the proposed AMPC method has better performance than the PI controller to address the frequency problem. At the same time, the proposed method has faster convergence speed and smaller overshoot from the enlarged plot in Fig. 7.

Figs. 8, 9, and 10 show the simulation results for case B. From the results, we can observe that the propose AMPC can address the frequency problem effectively when the large amount of renewable energy is imported in low-inertia circumstance from Fig. 8. The estimation parameters result in Fig. 9 shows that the UKF can estimate parameter with high accuracy. The estimation parameter T_a stables at almost 1.8s. The proposed AMPC has the faster response speed than that in case A to against the large fluctuation caused by large amount of PV and WT. However, the PI controller exhibits a instability performance from Fig. 10 due to the parameters of PI controller must be tuned when the system chrematistics are change.

Fig. 11 gives the total capital of PV, WT in case B. we can notice that the PI controller appears instability when the event occurs almost from 200s.

IV. CONCLUSIONS

This paper proposes a novel frequency regulation method based on AMPC for the MG system to address the frequency problem. The simulation results show that the proposed AMPC method can maintain the frequency stability of the MG system when large amount of renewable energy sources is imported and can effectively handle the frequency problem of the MG. Moreover, the comparative results show that the proposed method has higher response speed, robustness, and smaller overshoot to cope with the large disturbance than the PI controller. The proposed AMPC method can realise the automated optimal control regardless of changes in system characteristics. From the cost viewpoint, the proposed method can achieve low operating costs that could be a significant advantage for future MG construction.

REFERENCES

[1] M. Ranjian, and R. Shankar, "A literature survey on load frequency control considering renewable energy integration in power system: Recent trends and future prospects," Journal of Energy Storage, ELSEVIER, vol. 45,2022.

[2] J. Heidary, M. Gheisarnejad, H. Rastegar, and M. H. Khooban, "Survey on microgrids frequency regulation: Modeling and control systems," Electric Power Systems Research, ELSEVIER, vol. 213, 2022.

[3] N T. Mbungu, A A. Ismail, M. Aishabi, R C. Bansal, A. Elnady, and A K. Hamid, "Control and estimation techniques applied to smart microgrids: A review," Renewable and Sustainable Energy Reviews, ELSEVIER, vol. 179, 2023.

[4] I. Moschos, and C. Parisses, "A novel optimal PIλDND2N2 controller using coyote optimization algorithm for an AVR system," Engineering Science and Technology, an International Journal, ELSEVER, vol. 26, 2022.

[5] A. X. R. Irudayaraj, N. I. A. Wahab, M. Premkumar, M. A. M. Radzi, N. B. Sulaiman, V. Veerasamy, R. A. Farade, and M. Z. Islam, "Renewable sources-based automatic load frequency control of interconnected systems using chaotic atom search optimization," Applied Soft Computing, ELSEVIER, vol. 119, 2022.

[6] W. Chen, N. Sun, Z. Ma, W. Liu, and H. Dong, "A Two-Layer Optimization Strategy for Battery Energy Storage Systems to Achieve Primary Frequency Regulation of Power Grid," energies, vol. 16, No. 6, 2023.

[7] L. Xiong, X. Liu, H. Liu, and Yonghui Liu, "Performance Comparison of Typical Frequency Response Strategies for Power Systems With High Penetration of Renewable Energy Sources," IEEE Journal on Emerging and Selected Topics in Circuits and Systems, vol. 12, 2022, pp. 41-47.

[8] W. Wang, B. Yuan, Q. Sun, and R. Wennersten, "Application of energy storage in integrated energy systems — A solution to fluctuation and uncertainty of renewable energy," Journal of Energy Storage, ELSEVIER, vol. 52, 2022.

[9] H. H. Alhelou, N. Nagpal, N. Kassarwani, and Pierluigi Siano, "Decentralized Optimized Integral Sliding Mode-Based Load Frequency Control for Interconnected Multi-Area Power Systems," IEEE Access, vol. 11, 2023, pp. 32296-32307.

[10] X. Zhang, C. Li, B. Xu, Z. Pan, and Tao Yu, "Dropout Deep Neural Network Assisted Transfer Learning for Bi-Objective Pareto AGC Dispatch," IEEE Transactions on Power Systems, vol. 38, 2023, pp. 1432-1444.

[11] Z. Hu, S. Liu, W. Luo, and L. Wu, "Resilient Distributed Fuzzy Load Frequency Regulation for Power Systems Under Cross-Layer Random Denial-of-Service Attacks," IEEE Transactions on Cybernetics, vol. 52, No. 4, 2022, pp. 2396-2406.

[12] M. Adibi, and J. v. d. Woude, "Secondary Frequency Control of Microgrids: An Online Reinforcement Learning Approach," IEEE Transactions on Automatic Control, vol. 67, 2022, pp. 4824-4831.

[13] A. Cunillera, N. Bešinović, N v. Oort, and R M.P. Goverde, "Real-time train motion parameter estimation using an Unscented Kalman Filter," Transportation Research Part C: Emerging Technologies, ELSEVIER, vol. 143, 2022.

[14] S. Zhang, C. Zhang, S. Jiang, and X. Zhang, "A comparative study of different adaptive extended/unscented Kalman filters for lithium-ion battery state-of-charge estimation," Energy, ELSEVIER, vol. 246, 2022.

[15] S. Mokhtari, and K K. Yen, "Dynamic state estimation with additive noise for load frequency control using bilateral fuzzy adaptive unscented Kalman filter," Electric Power Systems Research, ELSEVIER, vol. 220, 2023.